

Optical sectioning using a digital Fresnel incoherent-holography-based confocal imaging system

ROY KELNER,* BARAK KATZ, AND JOSEPH ROSEN

Department of Electrical and Computer Engineering, Ben-Gurion University of the Negev, P.O. Box 653, Beer-Sheva 8410501, Israel

*Corresponding author: kelner@post.bgu.ac.il

Received 26 March 2014; revised 20 May 2014; accepted 27 May 2014 (Doc. ID 208919); published 1 August 2014

We propose a new type of confocal microscope using Fresnel incoherent correlation holography (FINCH). Presented here is a confocal configuration of FINCH using a phase pinhole and point illumination that is able to suppress out-of-focus information from the recorded hologram and hence combine the super-resolution capabilities of FINCH with the sectioning capabilities of confocal microscopy. © 2014 Optical Society of America

OCIS codes: (090.0090) Holography; (090.1995) Digital holography; (110.6880) Three-dimensional image acquisition; (180.1790) Confocal microscopy; (180.6900) Three-dimensional microscopy; (070.6120) Spatial light modulators.

<http://dx.doi.org/10.1364/OPTICA.1.000070>

Confocal imaging is commonly used for microscopy due to its ability to provide optical sectioning, improved contrast, and high-image resolution [1]. The concept of confocal microscopy was developed by Minsky in 1955 but found widespread use in biology only a few decades later. The reason for this delay is probably due to technological limitations at that time, as confocal imaging requires scanning over the entire imaged target [2,3]. Though confocal holographic systems that do not require scanning had been developed [4,5], they are unfortunately not suitable for fluorescence imaging [5], which is commonly practiced in microscopy for biological applications. In this Letter, we present, for the first time to our knowledge, a confocal configuration of Fresnel incoherent correlation holography (FINCH) [6]. FINCH is readily suitable for fluorescence microscopy and offers resolutions beyond the Rayleigh limit [7] but lacks the optical sectioning capabilities that are most important whenever thick objects are being imaged. These highly sought-after capabilities exist in the hereby proposed system and are achieved with the added cost of target

scanning. These costs, however, can be mitigated to a large degree if a proper scanning methodology is used [1,8].

Before discussing the proposed confocal FINCH system, the working concept of FINCH is first briefly presented. A schematic configuration of a dual-lens FINCH system [9,10] is shown in Fig. 1(a). It is assumed that the object is spatially incoherent; thus light beams that are emitted or scattered from two different object points cannot interfere with each other, and the system is analyzed by considering a single point source object. In Fig. 1(a), a spherical light beam is emitted from the source point a_o , located at the front focal plane of the objective lens L_o , and propagates into the FINCH system. An input polarizer $P1$ is set at a 45° angle to the active axis of a spatial light modulator (SLM), $SLM1$, which allows the formation of two in-parallel imaging systems in a common-path single-channel configuration. The SLM modulates the phase of only the polarization components of the beam that are in parallel to its active axis. Polarization components of the input beam that are perpendicular to its active axis are not modulated; for them, the SLM is a transparent element. The system can thus be considered as two imaging systems, each acting with one of two orthogonal polarization components of light. In these systems, the input beam of light is collected by the objective lens L_o and then further concentrated by the lens L_c . In one of the two systems the SLM does not influence the beam, and an image is formed at the image point a_2 ; in the other, a converging diffractive lens is displayed on $SLM1$ and the beam is concentrated into the image point a_1 .

To record a hologram of the maximum achievable resolution [7,9], a charge-coupled device (CCD) is positioned between the two image points, a_1 and a_2 , so that a perfect overlap is achieved between the beam diverging from the image point a_1 and the beam converging toward the image point a_2 . Note that interference can occur between these two beams, since they originate from the same point source, a_o , granted that the maximal optical path difference between the two is shorter than the coherence distance of the light source [9]. Further, note that the output polarizer $P2$ is essential and is used

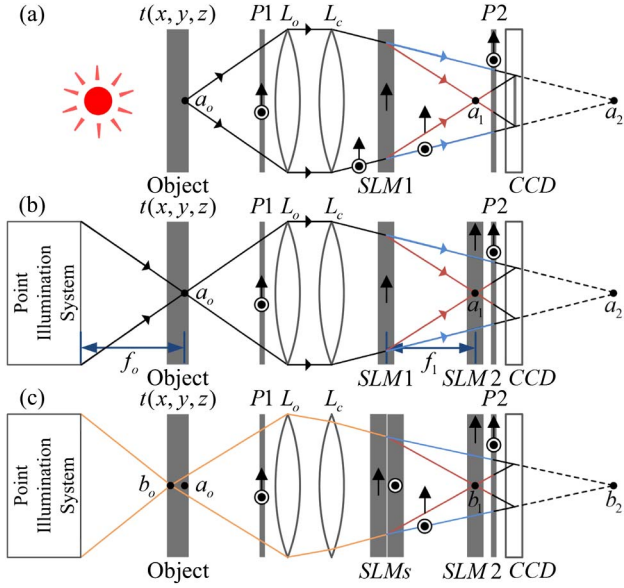


Fig. 1. Schematics of FINCH recorders: (a) a dual-lens FINCH system; (b), (c) the proposed confocal FINCH systems. $P1$ and $P2$, polarizers; L_o , objective lens; L_c , converging lens; $SLM1$ and $SLM2$, spatial light modulators; CCD , charge-coupled device.

to project the polarization components of the two beams into a common orientation. Usually, $P2$ is also set at a 45° angle to the active axis of $SLM1$, but other angles can be used to control the relative intensity of the two beams [11]. The intensity of the two-beam interference pattern is recorded by the CCD, giving rise to a 0th order term and two other terms attributed to the holographic image of a_o and its twin. A phase-shifting procedure [6,7,9–11], utilizing $SLM1$, requires at least three exposures and is performed so that only the holographic image term remains. The spatial incoherence of the object ensures that the final recorded FINCH hologram is a summation over the intensities of all point source interference patterns. The recorded object can then be reconstructed from the hologram through a digital Fresnel propagation to a specific reconstruction distance, z_r [9]. An additional feature of FINCH is that out-of-focus points are also recorded in the hologram. This, on one hand, can be advantageous when re-focusing to planes of different depths is required, but on the other hand, it can impose noise and artifacts over the observed in-focus image. Next, we present a FINCH-based method that can section any desired plane out of the three-dimensional (3D) object distribution.

In a confocal FINCH system [Fig. 1(b)], a second SLM, $SLM2$, is positioned in the x y plane in which the image point a_1 is formed. A diffractive optical element, hereby referred to as a “phase pinhole,” is displayed on $SLM2$. This phase pinhole is considered as one of the main innovations of the presented work. The phase pinhole at the scanning point (m, n) is described by the following equation:

$$G(\vec{r}; \vec{r}_l) = \begin{cases} \exp(i\varphi_k) & |\vec{r} - \vec{r}_l - \vec{r}_s| \leq r_1 \\ \exp(i\alpha|\vec{r} - \vec{r}_l - \vec{r}_s|)P(\vec{r}/R_2) & \text{Otherwise} \end{cases}, \quad (1)$$

with $\vec{r} = (x, y)$, $\vec{r}_l = (am, bn)$, and $\vec{r}_s = (x_s, y_s)$, and is composed of the actual pinhole part, $\exp(i\varphi_k)$, which is a circular area of radius r_1 set to a uniform phase modulation, surrounded by a mask of an axicon, $\exp(i\alpha r)$, where α is a parameter proportional to the axicon angle, $P(\vec{r}/R_2)$ denotes the circular aperture of $SLM2$, with a clear disk of radius R_2 , a and b are scanning intervals in the x and y axes, respectively, and \vec{r}_s is the starting point of the scanning. In the confocal FINCH system, for every scanning point (m, n) , the uniform phase modulation at the pinhole region is set to three different φ_k values, usually 0° , 120° , and 240° , and $SLM1$ is no longer used for the phase-shifting procedure. Since the phase is changed only within the phase pinhole, any information carried by a wave that passes through $SLM2$ outside the phase pinhole and does not eventually interfere with the wave modulated by the phase pinhole is lost after the phase-shifting procedure. Overall, the proposed phase pinhole can be considered as a regular pinhole for the polarization components parallel to the active axis of $SLM2$ and as a clear aperture (of $SLM2$ dimensions) for the orthogonal polarization components. Accordingly, the proposed phase pinhole can perform properly even without displaying an axicon. Yet, by incorporating the axicon, light outside of the circular pinhole is actually deflected outside the sensor area. This, in turn, diminishes the amount of light that would otherwise reach the CCD and is only later removed digitally via phase shifting. Thus, the dynamic range of the CCD can be better exploited when the axicon is present. Eventually, we are left mostly with the information of the interference between light that passes through the phase pinhole of $SLM2$, with its orthogonal counterparts that are imaged at the point a_2 .

The above described phase pinhole can efficiently achieve optical sectioning, as will be demonstrated promptly. However, better results can be achieved by incorporating a point illumination system, forming a complete confocal FINCH system. In a confocal FINCH system [Fig. 1(b)], the object points outside the scanning spot are eliminated from the recorded hologram. First, due to the point illumination, any of the object points that are not lit (i.e., are not within the cone of light) will not be recorded. Second, all points that are focused onto the region of $SLM2$ but fall outside of the phase pinhole are also rejected from the hologram. Points that fall partly within the phase pinhole will be attenuated in the recorded hologram, as their recorded fringe patterns will have a very limited aperture, rejecting most of their intensity. Most importantly, points whose images are out of focus on $SLM2$ are either completely eliminated from the recorded hologram (if their light does not propagate through the phase pinhole) or their intensity is greatly diminished, first due to the out-of-focus illumination and then due to an additional rejection of most of the information, since only a small part of their cone of light can propagate through the phase pinhole. This mechanism allows optical sectioning, with a tradeoff; unlike a regular FINCH system [Fig. 1(a)], which records holograms that contain the complete 3D information of the wide-field illuminated scene, here only a single point in space is properly imaged in a single

recorded hologram, and thus a scanning mechanism is required over the entire object.

Scanning of the entire object can be performed either mechanically, by translating the object in the x , y , and z axes, or electronically, without any mechanical intervention. In order to electronically control the position of the point illumination, one can introduce into the illumination system an additional SLM, for example, or other beam steerers (acousto-optical or electro-optical). As the object is scanned over the x y plane, the imaged point over *SLM2* is formed at different positions, and so the phase pinhole mask is electronically centered to that point. For each scanning position (m, n) , a single hologram is recorded (extracted from three exposures by a complete phase-shifting procedure). From each hologram a single point is reconstructed using the Fresnel diffraction integral formula for a single output point (a complete convolution is unnecessary), and all points from all of the recorded holograms can then be combined into a single image. Alternatively, as performed in the reported experiments, from each hologram a reconstruction of the entire input plane can be calculated; then, for each single pixel of the hologram, the maximum intensity value from all reconstructions is chosen, and a complete reconstruction of a specific x y plane is formed. In practice, just like in conventional confocal microscopy [1,8], many points can be imaged in parallel. This can be achieved, for example, by point illuminating multiple points on the same x y plane simultaneously, while a phase pinhole mask of multiple pinholes is displayed over *SLM2*. Of course, the distance between the illuminated points must be chosen so that proper optical sectioning can be achieved.

It is also possible to electronically scan at different depths (z positions) by controlling the focal length of the converging lens displayed on *SLM1*, but this will not allow a perfect overlap of the interfering beams on the CCD plane, and thus a resolution reduction is expected. A mechanical movement of the object at the z axis may then be preferred. This is a bearable cost, since this movement is only necessary once an x y plane scan is completed. Note that alternative FINCH configurations can be used to achieve perfect overlap at different z distances without a mechanical movement. This can be achieved by incorporating another SLM, placed with its active axis perpendicular to the active axis of *SLM1* [see Fig. 1(c), in which two SLMs are stacked together and a perfect overlap can be achieved for any desired point source object]. This SLM can even replace the lens L_c if needed.

In Fig. 1(b), the point a_o is located on the optical axis and on the back and front focal planes of the point illumination system and the objective lens, respectively. Consider an arbitrary point located on the optical axis at a distance z_o from a_o . According to McCutchen's theorem, the complex amplitude at that point, $(0, 0, z_o)$, is given by $h_{\text{ill}}(z_o) = \mathcal{F}\{H_{\text{ill}}(2\lambda f_o^2 \rho)\}$, where the right-hand-side term is attributed to a one-dimensional Fourier transform of the radial aperture distribution H_{ill} , of the illumination system, f_o is its focal distance, λ is the central wavelength, and ρ is the variable of H_{ill} equal to r^2 [12]. The point $(0, 0, z_o)$ is imaged into two image points, $(0, 0, z_1 = z_o m_{a,1})$ and $(0, 0, z_2 = z_o m_{a,2})$, with complex

amplitudes of $b_1 h_{\text{ill}}(z_o)$ and $b_2 h_{\text{ill}}(z_o)$, respectively, where b_1 and b_2 are constants, $m_{a,1}$ and $m_{a,2}$ represent the axial magnifications of the corresponding imaging systems, and the planes of $z_{1,2} = 0$ are at the imaged points a_1 and a_2 , respectively. The waves associated with these two points interfere on the CCD plane, forming a fringe pattern from which the point $(0, 0, z_o)$ can be reconstructed. The interference pattern can be described as

$$I = \left| c_1 e^{i\phi_k} Q\left(\frac{1}{l_1}\right) h_{\text{ill}}(z_o) h_{\text{det}}(m_{a,1} z_o) + c_2 Q\left(\frac{1}{-l_2}\right) h_{\text{ill}}(z_o) \right|^2, \quad (2)$$

where $Q(1/l_k) = \exp[i\pi l_k^{-1} \lambda^{-1} (x^2 + y^2)]$ is a quadratic phase function. The left-hand-side term in Eq. (2) is attributed to the wave associated with the image point $(0, 0, z_1 = z_o m_{a,1})$, a distance l_1 from the CCD, following its multiplication by the phase mask of the form of Eq. (1), which effectively multiplies the wave by a complex amplitude proportional to $h_{\text{det}}(z_1) = \mathcal{F}\{H_{\text{det}}(2\lambda f_1^2 \rho)\}$, with H_{det} affiliated with the imaging system forming that point and f_1 as its focal distance. Note that in the case of clear circular apertures, H_{ill} and H_{det} are Rect functions, so h_{ill} and h_{det} are Sinc functions. The right-hand-side term in Eq. (2) is attributed to the wave associated with the image point $(0, 0, z_2)$, a distance l_2 from the CCD.

Following a phase-shifting procedure, only one of the cross terms in Eq. (2) is left:

$$H(x, y) = c_o Q\left(\frac{1}{z_r}\right) h_{\text{ill}}(z_o) h_{\text{ill}}^*(z_o) h_{\text{det}}(m_{a,1} z_o) P(\vec{r}/R_H), \quad (3)$$

where $\vec{r} = (x, y)$, $z_r = l_1 l_2 / (l_1 + l_2)$ is the reconstruction distance and $P(\vec{r}/R_H)$ denotes the circular aperture of the hologram, with a clear disk of radius R_H . This radius is determined by the overlap area of the two interfering waves. The recorded point can then be reconstructed from the hologram through a digital Fresnel propagation to the reconstruction distance z_r [9]:

$$\begin{aligned} h(u, v; z_o) &= H(x, y) * Q\left(\frac{1}{z_r}\right) \propto \\ &h_{\text{ill}}(z_o) h_{\text{ill}}^*(z_o) h_{\text{det}}(m_{a,1} z_o) \mathcal{F}\{P(\lambda z_r \vec{r}/R_H)\} \propto \\ &|h_{\text{ill}}(z_o)|^2 h_{\text{det}}(m_{a,1} z_o) J_{\text{inc}}\left(\frac{2\pi R_H}{\lambda z_r} \sqrt{u^2 + v^2}\right), \quad (4) \end{aligned}$$

where $*Q(1/z_r)$ denotes a Fresnel propagation (here, $*$ denotes a two-dimensional convolution) and $J_{\text{inc}}(r) \triangleq J_1(r)/r$ is the Bessel function of the first kind and of order one. Comparing Eq. (4) above with Eq. (5) of Ref. [9], we conclude that the transverse resolution of the proposed system, attributed to the J_{inc} term, is similar to a regular FINCH system; however, the longitudinal separation is much better in the proposed system and is comparable to that of a conventional confocal microscope, due to the z_o -dependent terms $|h_{\text{ill}}(z_o)|^2 h_{\text{det}}(m_{a,1} z_o)$.

In order to demonstrate the optical sectioning capabilities of the proposed system, the experimental setup described in Fig. 2

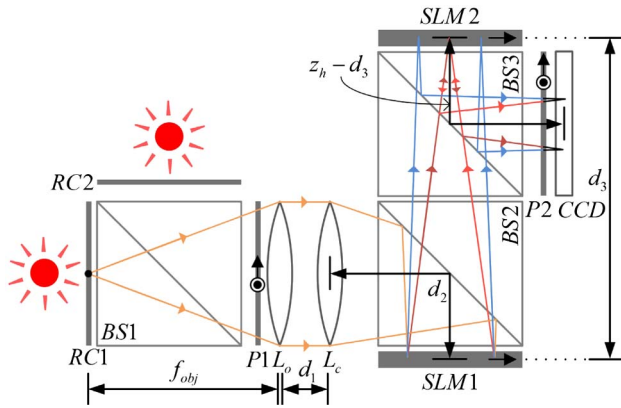


Fig. 2. Experimental setup: $RC1$ and $RC2$, resolution charts; $BS1$, $BS2$, and $BS3$, beam splitters; $P1$ and $P2$, polarizers; L_o , objective lens; L_c , converging lens; $SLM1$ and $SLM2$, spatial light modulators; CCD , charge-coupled device.

was used. A beam splitter, $BS1$, was used as a beam combiner, with two resolutions charts (negative National Bureau of Standards 1963A), $RC1$ and $RC2$, positioned at a distance of 30 and 31 cm (for the x y plane scan of $RC1$) or 29 and 30 cm (for the scan of $RC2$) away from the objective lens, respectively. Together, the two charts can be considered as a 1 cm thick object. The resolution charts were back-illuminated using two LEDs (Thorlabs LED635L, 170 mW, $\lambda = 632.8$ nm, $\Delta\lambda = 15$ nm). Diffuser sheets were attached to the charts in order to imitate a scattering/illuminating object. The focal lengths of the objective lens L_o and the lens L_c were chosen as $f_{obj} = 30$ cm and $f_c = 150$ cm, respectively. For simplicity, we have replaced these two lenses with an equivalent lens with a focal length of $f_e = 25$ cm, implying that $d_1 = 0$ cm (Fig. 2). Other parameters in the system were: $d_2 = 10$ cm, $d_3 = 66.3$ cm, and $z_h = 90$ cm (which is the distance from $SLM1$ to the CCD and is the parameter that determines the transverse magnification of FINCH as $M_T = z_h/f_{obj}$). The two SLMs (Holoeye PLUTO, 1920×1080 pixels, $8 \mu\text{m}$ pixel pitch, phase-only modulation) were positioned at similar orientations, with their active axes in parallel, while the two polarizers, $P1$ and $P2$, were set at a 45° angle to these axes, and in parallel to each other. Since the two SLMs are reflective, two beam splitters, $BS2$ and $BS3$, were incorporated into the system so that the two SLMs were positioned orthogonally to the optical axis. This causes a loss of a large amount of light, which can be avoided by either by positioning the SLMs at a small angle, eliminating the beam splitters but requiring a careful compensation in the SLM displayed masks, or by using transmissive components (e.g., $SLM1$ can be replaced with a liquid crystal gradient index lens [13]).

In the experiments, we compared the results of a regular FINCH system (setting the phase mask of $SLM2$ to a constant zero modulation) and an optical sectioning FINCH system (with a phase pinhole displayed on $SLM2$). The phase pinhole radius was $r_1 = 44 \mu\text{m}$, surrounded by an axicon of parameter $\alpha = 2\pi \cdot 13 \cdot 10^{-3}/\lambda$, and the scanning over a grid of size 81×61 points on each plane was performed with pinhole displacements in the x and y axes of $40 \mu\text{m}$. The exposure time

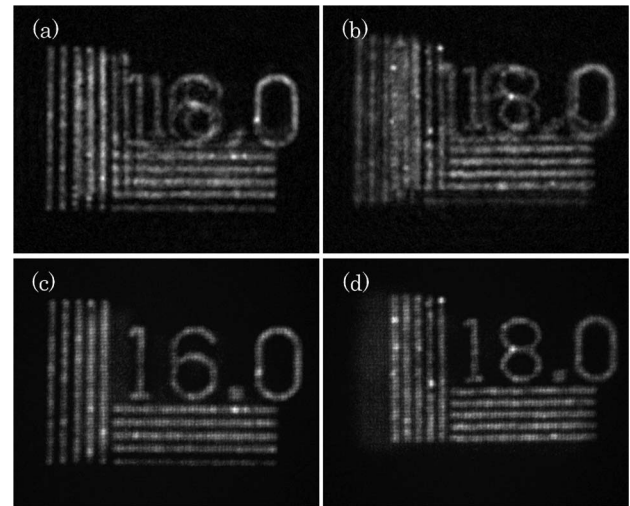


Fig. 3. Experimental results: (a) FINCH reconstruction of a 16.0 cycles/mm resolution chart located 30 cm away from the objective lens, with the 18.0 cycles/mm resolution chart at 31 cm; (b) FINCH reconstruction of a 18.0 cycles/mm resolution chart located 30 cm away from the objective lens, with the 16.0 cycles/mm resolution chart at 29 cm; (c), (d) the optical sectioning FINCH equivalents of (a) and (b), respectively.

was set to 1.25 s, implying a scanning time of roughly 5 h per plane. Note that in the reported experiments we do not use the proposed point illumination, and the entire object is illuminated at all times. This is to emphasize the contribution of the phase pinhole, which can be considered the most genuine part and newest contribution of this work, whereas scanning illumination systems are widely used in confocal microscopy [8]. It should be noted that such systems, in which the sectioning is performed solely by the phase pinhole, can be useful for imaging situations in which the observed scene cannot be illuminated as required.

The experimental results are presented in Fig. 3. Reconstruction results from regular FINCH holograms are presented in Figs. 3(a) and 3(b), for the resolution targets closest to the objective ($RC1$) and farthest from it ($RC2$), respectively. Here, the out-of-focus targets greatly diminish the quality of the reconstruction. The equivalents of the reconstructions of Figs. 3(a) and 3(b), resulting from the phase-pinhole-incorporated FINCH, are presented in Figs. 3(c) and 3(d), respectively. Unlike regular FINCH holography, the out-of-focus targets are highly attenuated, and so the in-focus targets appear with much detail, high contrast, and weak background artifacts. Hence, the optical sectioning capability of the proposed system is clearly demonstrated. It should be noted that once a single point illumination is incorporated into the system, the sectioning capabilities are expected to be further enhanced. Here, the out-of-focus target is illuminated with similar intensity to the in-focus target, unlike the case of point illumination, where object points will exhibit an illumination of less intensity that declines farther away from the location of the illuminated point.

To conclude, a new confocal FINCH configuration capable of optical sectioning has been proposed in this Letter, and a

simpler configuration of FINCH capable of sectioning has been demonstrated and compared with regular FINCH. The proposed system combines the super-resolution capabilities of FINCH with the sectioning capabilities of confocal microscopy. Together with the notable capabilities of FINCH for fluorescent microscopy, parallel illumination arrangements, and nonmechanical scanning schemes [8], we expect the proposed system to have an important role in microscopy in general and biological microscopy in particular. Other potential applications for the proposed system might include high lateral resolution tomography that is also capable of simultaneous imaging of passive reflecting surfaces and fluorescent objects.

FUNDING INFORMATION

National Institutes of Health (NIH) (U54GM105814); The Israel Ministry of Science and Technology (MOST); The Israel Science Foundation (ISF) (439/12).

REFERENCES

1. R. H. Webb, *Rep. Prog. Phys.* **59**, 427 (1996).
2. M. Minsky, *Scanning* **10**, 128 (1988).
3. W. B. Amos and J. G. White, *Biol. Cell* **95**, 335 (2003).
4. P.-C. Sun and E. N. Leith, *Appl. Opt.* **33**, 597 (1994).
5. R. Chmelik and Z. Harna, *Opt. Eng.* **38**, 1635 (1999).
6. J. Rosen and G. Brooker, *Opt. Lett.* **32**, 912 (2007).
7. J. Rosen, N. Siegel, and G. Brooker, *Opt. Express* **19**, 26249 (2011).
8. P. J. Verveer, Q. S. Hanley, P. W. Verbeek, L. J. Van Vliet, and T. M. Jovin, *J. Microsc.* **189**, 192 (1998).
9. B. Katz, J. Rosen, R. Kelner, and G. Brooker, *Opt. Express* **20**, 9109 (2012).
10. R. Kelner, J. Rosen, and G. Brooker, *Opt. Express* **21**, 20131 (2013).
11. G. Brooker, N. Siegel, V. Wang, and J. Rosen, *Opt. Express* **19**, 5047 (2011).
12. C. W. McCutchen, *J. Opt. Soc. Am.* **54**, 240 (1964).
13. G. Brooker, N. Siegel, J. Rosen, N. Hashimoto, M. Kurihara, and A. Tanabe, *Opt. Lett.* **38**, 5264 (2013).